[15] NMR Techniques Used with Very Large Biological Macromolecules in Solution

By GERHARD WIDER

Abstract

Methods for the characterization of very large biological macromolecules by NMR in solution are presented. For studies of molecular structures with molecular weights beyond 100,000 Da transverse relaxation in common multidimensional NMR experiments becomes a limiting factor. Novel techniques optimize transverse relaxation based on cross-correlated relaxation between dipole–dipole interactions and chemical shift anisotropy (CSA), and include transverse relaxation-optimized spectroscopy (TROSY), cross-correlated relaxation-enhanced polarization transfer (CRINEPT), and cross-correlated relaxation-induced polarization transfer (CRIPT). In combination with various biochemical isotope-labeling techniques these experimental schemes make possible studies of biological macromolecules with molecular masses of up to 1,000,000 Da by NMR in solution. The physical basis and the implementation of the experiments are discussed.

Introduction

The foundations of successful applications of nuclear magnetic resonance (NMR) spectroscopy are high-quality spectra recorded with good sensitivity and spectral resolution. With increasing molecular weight these basic requirements are harder to achieve. The scarcity of NMR studies with biological macromolecules above 30 kDa molecular weight reflects the increasing challenge and costs involved. During the past years, considerable effort has been devoted to extend applications of NMR in solution to larger molecular systems (Pervushin *et al*., 1997; Riek *et al*., 1999; Tugarinov and Kay, 2003; Tugarinov *et al*., 2003; Wider and Wüthrich, 1999; Wüthrich and Wider, 2003). The availability of such NMR techniques is of considerable interest, for example, for structural investigations of larger proteins that

0076-6879/05 $35.00

resist crystallization, or for studies of intermolecular interactions in solution involving large molecules and supramolecular assemblies including structure–activity relationships (SAR) by NMR (Shuker *et al.*, 1996).

When studying large molecules and macromolecular assemblies in solution by conventional NMR methods, usually a number of problems arise: (1) extensive signal overlap due to the high complexity of the spectra, (2) low solubility of the solute limits the sensitivity, and (3) low sensitivity and line broadening due to rapid transverse spin relaxation. Spectral overlap can be reduced with a variety of techniques that result in a simplification of spectra: e.g., fractional deuteration (Gardner and Kay, 1998; Lian and Middleton, 2001), amino acid selective labeling (Kainosho, 1997), and segmental labeling (Xu *et al.*, 1999; Yamazaki *et al.*, 1998; Yu, 1999). The limitations caused by low solubility and transverse relaxation pose severe technical challenges. However, advances have been achieved with both NMR hardware and novel NMR techniques. The recent development of NMR cryogenic probes improved the sensitivity of NMR measurements by a factor of 3, and novel experimental approaches, in particular TROSY (transverse relaxation-optimized spectroscopy) (Pervushin *et al.*, 1997), CRINEPT (cross-correlated relaxation-enhanced polarization transfer) (Riek *et al.*, 1999) and CRIPT (cross-correlated relaxation-induced polarization transfer) (Brüschweiler and Ernst, 1992; Dalvit, 1992; Riek *et al.*, 1999), extended the size limit for observation of NMR signals in solution severalfold. These experimental techniques use spectroscopic means to reduce transverse relaxation, making possible studies of molecular systems with molecular weights up to 1000 kDa (Fiaux *et al.*, 2002). The introduction of the novel techniques opens a wide range of new applications for NMR in solution, in particular in the newly emerging field of structural and functional genomics. In the following sections these new techniques for observation of high-quality NMR spectra with molecular sizes beyond 100 kDa are discussed.

Optimizing Transverse Relaxation

Transverse relaxation has a large impact on the quality of NMR spectra. With increasing molecular weight, transverse relaxation becomes larger. Consequently, the resonance lines become broader and the sensitivity decreases. A few years ago TROSY was introduced (Pervushin *et al.*, 1997) and in the meantime has found widespread applications (Fernández and Wider, 2003), since better spectra are readily obtained when working with molecular sizes above 15–20 kDa. The TROSY technique can reduce the effective relaxation of the measured signal during the pulse sequence and during the data acquisition resulting in increased spectral resolution and improved effective sensitivity. The detailed understanding of the

TROSY principle requires relaxation theory based on quantum mechanical principles (e.g., Goldman, 1984; Pervushin, 1997, 2000). Here, a simplified approach based on classic physics shall advance a more intuitive understanding.

In the following TROSY is discussed using the important example of a ^{15}N and a ^{1}H nucleus, such as in ^{15}N–^{1}H amide groups of proteins or in nucleic acid bases. Both nuclei have a spin-$\frac{1}{2}$, which can classically be described by a magnetic dipole having two orientations: up and down. In the ^{1}H-NMR spectrum a doublet is observed originating from the protons attached to ^{15}N nuclei with spin up and spin down, respectively. These doublets are routinely collapsed into a single, centrally located line by decoupling (Bax and Grzesiek, 1993; Wider, 1998), with the expectation of obtaining a simplified spectrum and improved sensitivity. However, in the spectrum of a large protein the individual multiplet components have different linewidths (Pervushin *et al*., 1997). Decoupling mixes the different relaxation rates that deteriorate the averaged signal for large molecules studied at high magnetic fields. In TROSY no decoupling is applied, and only the narrowest, most slowly relaxing line of each multiplet is retained. TROSY disregards half of the potential signal of an amide moiety. This loss is compensated in large molecules by the slower relaxation of the selected resonance line.

Why do the individual components of the ^{1}H–^{15}N doublet have different relaxation rates for large molecules? The answer requires an analysis of the magnetic fields created by different interactions. These fields become time dependent (and cause relaxation) due to stochastic rotational motions of the molecule containing the amide group. Fortunately, for large proteins only the z-component of the stochastic magnetic fields contributes significantly to transverse relaxation (''dephasing'' of the signals), because the molecules rotate too slowly to create the necessary frequency components at the transition frequencies. In the context of relaxation theory, the z-components correspond to terms with spectral density at zero frequency. In the amide moiety two processes lead to significant relaxation: dipole–dipole (DD) and chemical shift anisotropy (CSA) interactions. Individually, the two relaxation processes do not cause differential relaxation either for the two-proton or for the two-nitrogen transitions. The DD and CSA interactions are present simultaneously and their magnetic fields add. This addition leads to larger and smaller z-components, since the dipolar field (but not CSA) has an opposite sign depending on the state of the attached nucleus. Consequently, the relaxation rates of the two transitions are potentially different. However, this static picture presents just a snapshot that can influence relaxation only if the stochastic magnetic fields created by DD interactions and CSA have the same dependence on the rotational motion of the molecules (Goldman, 1984; Pervushin *et al*., 1997).

The field created by the nuclear dipole depends on $(3\cos^2\theta - 1)$, where θ is the angle between the main magnetic field and the direction of the H–N bond in an amide moiety, all other factors being constant. For the magnetic field caused by CSA, the same angular dependence is obtained when an axially symmetric CSA tensor with its main axis along the H–N bond is assumed (Pervushin *et al.*, 1997). As a result, the differential stochastic magnetic fields are maintained irrespective of the molecular tumbling, which leads to different relaxation rates for individual transitions. With increasing strength of the main magnetic field, CSA relaxation increases whereas DD relaxation stays constant. The optimal TROSY effect can thus be obtained by choosing the appropriate field strength. Interestingly, in an amide moiety the TROSY effect for both the ^{1}H and the ^{15}N nuclei has an optimum at about the same magnetic field strength, which is approximately 23.5 T, corresponding to a proton resonance frequency of 1000 MHz (Pervushin *et al.*, 1997). In experiments with ^{1}H and ^{15}N nuclei, the slower relaxing component for both nuclei is selected in a relaxation-optimized experiment.

The fact that amide groups are strategically located in the polypeptide backbone of proteins and in the bases of nucleotides of DNA and RNA molecules makes them a prime target in the optimization of many NMR experiments with biological macromolecules. In practice, complete cancellation of relaxation cannot be expected. In particular, the principal tensor axis of the CSA tensor and the ^{15}N–^{1}H bond is not colinear, and the properties of the CSA tensor vary from residue to residue (Fushman and Cowburn, 1999). In addition, there is some residual transverse relaxation that cannot be influenced by TROSY, especially dipole–dipole couplings with ''remote'' protons, i.e., all protons outside of the ^{15}N–^{1}H group. Therefore, an optimal TROSY effect is obtained with uniformly deuterated proteins, where remote couplings are limited to nearby amide protons.

TROSY is not limited to amide moieties in biological macromolecules; important applications use CH-groups in aromatic rings (Brutscher *et al.*, 1998; Pervushin *et al.*, 1998), where large signal enhancement could be obtained. More recently, a TROSY experiment for the carbon nuclei in methyl groups was described (Tugarinov *et al.*, 2003). In a [^{13}C,^{1}H]-HMQC (heteronuclear multiple-quantum correlation) experiment, the methyl carbon is in a multiple quantum state with one proton, which eliminates their mutual dipolar interactions, and for half of the carbon nuclei the other two attached protons have opposite spin states. Thus, their dipolar fields at the carbon nuclei cancel each other in large molecules.

Optimizing Polarization Transfer

In nearly all multidimensional NMR experiments for studies of biological macromolecules in solution, magnetization is transferred from

one type of nucleus to another via scalar spin–spin couplings using INEPT (insensitive nuclei enhanced by polarization transfer) pulse sequences (Morris and Freeman, 1979). With increasing molecular weight, transverse relaxation during the INEPT transfer period becomes a limiting factor that severely compromises sensitivity. On the other hand the performance of the previously little-used CRIPT improves for larger molecules (Brüschweiler and Ernst, 1992). The novel technique CRINEPT (Riek *et al*., 1999) combines CRIPT (Dalvit, 1992) and INEPT. For even larger molecular weights, polarization transfer using only CRIPT will become an alternative to CRINEPT. CRIPT and CRINEPT make use of the same cross-correlated relaxation, which is the basis for TROSY. Thus for amide groups the optimal magnetic field strength for these polarization transfer mechanisms corresponds to 1 GHz proton resonance frequency.

The INEPT and CRIPT transfer elements are compared in Fig. 1. In INEPT, antiphase magnetization is created via J-coupling during the period τ_1. In CRIPT, the effect of the J-coupling is refocused by omitting the 180° nitrogen pulse in the transfer period τ_2, and antiphase magnetization is obtained solely via cross-correlated relaxation. Ideally the fast relaxing doublet component has completely relaxed during τ_2, whereas the slowly relaxing component has hardly been reduced. This situation is indicated in Fig. 1 by the stick patterns that visualize the doublet appearance at the beginning and at the end of the transfer period at time points *a* and *b*, respectively. The asymmetric doublet at the end of the CRIPT transfer period τ_2 can be decomposed into a sum of an in-phase and an antiphase doublet with half the intensity of the original resonance line. In a physical sense this view represents another basis set describing the same situation. However, this basis visualizes that via cross-correlated relaxation at most half the magnetization arrives in an antiphase state and is the basis for the polarization transfer. The same result is obtained with a rigorous quantum mechanical calculation (Brüschweiler and Ernst, 1992). Similar to the situation with TROSY, for large proteins half the magnetization with optimized relaxation may easily surpass the magnetization obtained with averaged relaxation during the transfer period in an INEPT sequence.

Figure 2 shows three experimental schemes that make use of CRINEPT and CRIPT magnetization transfer elements: two-dimensional (2D) [^{15}N,^{1}H]-CRINEPT-TROSY, 2D [^{15}N,^{1}H]-CRINEPT-HMQC-[^{1}H]-TROSY, and 2D [^{15}N,^{1}H]-CRIPT-TROSY (Riek *et al*., 1999). Note that all three schemes use water flip-back pulses that keep the water polarization close to its equilibrium value during the whole experiment. This is a requirement when working with very large proteins (see next section). The 2D [^{15}N,^{1}H]-CRINEPT-TROSY experiment (Fig. 2A) consists of three time periods τ used for polarization transfer and for the selection of the fastest and the

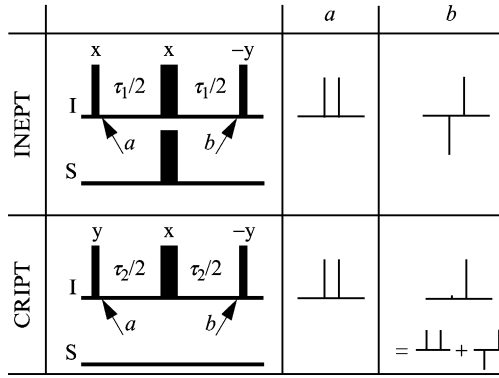

FIG. 1. Representation of two different magnetization transfer elements between nuclei I and S. The pulse sequence segments for an INEPT and a CRIPT transfer are shown along with stick patterns characterizing the doublet signal of spin I at the beginning and at the end of the transfer period at time points *a* and *b*, respectively (assuming no relaxation in INEPT and ideal cross-correlated relaxation in CRIPT). The narrow and wide vertical bars indicate 90° and 180° pulses that are applied at the resonance frequency of the I and S spins, respectively; the phase is *x* unless indicated otherwise above the pulse bar; note the difference in phase of the first pulse in the two-pulse sequence fragments. In INEPT the in-phase doublet evolves into an antiphase signal under J coupling. In CRIPT the evolution under J coupling is refocused and one component of the doublet relaxes much faster; the remaining pattern can alternatively be viewed as a sum of an in-phase and of an antiphase signal with each having half the intensity. The time period τ_1 depends on the scalar coupling between the two nuclei I and S. J_{IS}: $\tau_1 = 1/(2 J_{IS})$; the time period τ_2 depends on the molecular size and has to be estimated from build-up measurements (Fig. 4); τ_2 can be as short as 1 ms for extremely large molecules.

most slowly relaxing multiplet components, which is in contrast to TROSY, where only the narrowest component is selected. In practice, the additional component relaxes so fast that it is often not detectable. In CRINEPT transverse relaxation optimization is active during all three time periods τ and during the evolution and acquisition periods, t_1 and t_2; in other words, the experiment is fully optimized for relaxation. This implementation of CRINEPT has the disadvantage that the combination of INEPT- and CRIPT-type magnetization transfer causes chemical shift evolution of the proton signals during the first period τ, which cannot be refocused; consequently, half the signal is lost.

The 2D [^{15}N,^{1}H]-CRINEPT-HMQC-[^{1}H]-TROSY (Fig. 2B) is an alternative to the 2D [^{15}N,^{1}H]-CRINEPT-TROSY. The conventional [^{15}N,^{1}H]-HMQC experiment (Müller, 1979) contains two CRINEPT-type transfers. To make the sequence useful for large molecules it needs a few important changes. The transfer periods have to be optimized for CRINEPT transfer; no heteronuclear decoupling during acquisition must be applied, and water

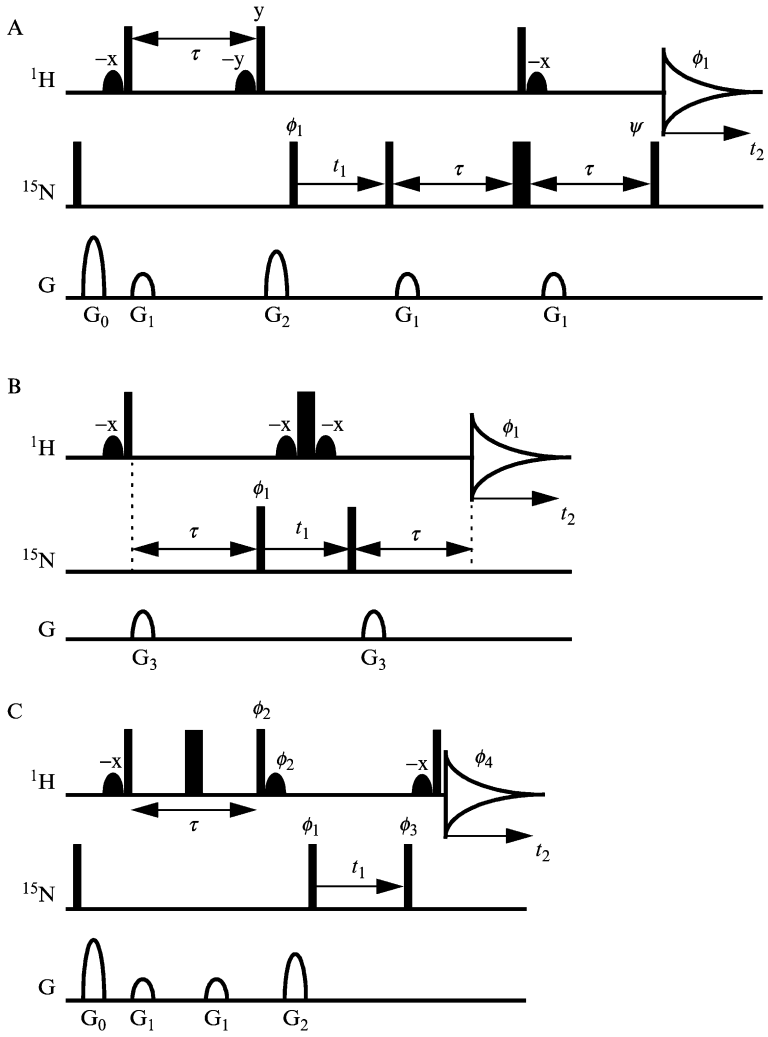

FIG. 2. [^{15}N, ^{1}H] correlation experiments using cross-correlated relaxation for magnetization transfer. (A) 2D [^{15}N,^{1}H]-CRINEPT-TROSY, (B) 2D [^{15}N,^{1}H]-CRINEPT-HMQC-[^{1}H]-TROSY, and (C) 2D [^{15}N,^{1}H]-CRIPT-TROSY. The narrow and wide vertical bars indicate 90° and 180° pulses, respectively, which are applied at the proton (^{1}H) and nitrogen (^{15}N) frequencies with phase *x* unless indicated otherwise above the pulse bar. Bell shapes on the ^{1}H line represent selective 90° pulses on the water resonance (duration ~1 ms), which keep the water magnetization along the positive *z*-axis during the whole experiment. On the line marked G, open bell shapes indicate pulsed magnetic field gradients applied along the *z*-axis with the following approximate durations and strengths: G_0, 1 ms, 30 G/cm; G_1, 300 μs, 20 G/cm; G_2, 400 μs, 40 G/cm, G_3, 800 μs, 10 G/cm. In (A) and (C) the magnetization of

flip-back pulses have to be introduced (see next section). Compared to [^{15}N,^{1}H]-CRINEPT-TROSY, there are only two periods τ and there is no signal loss due to proton chemical shift evolution before detection of the signal. However, there is no TROSY during the evolution period t_1 where the spins are in a multiple quantum state, which results in faster relaxation. In general, the experiment will have higher overall sensitivity but lower resolution in the indirect dimension than the [^{15}N,^{1}H]-CRINEPT-HMQC-[^{1}H]-TROSY. The sequence does not contain any selection of multiplet components and the resonances are split in the proton dimension due to scalar coupling. Again, in practice the broader component is often not visible in the spectra due to its fast relaxation.

For molecular structures with rotational correlation times longer than 120 ns, i.e., molecular weights larger than 300 kDa, the 2D [^{15}N,^{1}H]-CRIPT-TROSY experiment finds application (Fig. 2C). The scheme is fully optimized for transverse relaxation and uses cross-correlated relaxation for the polarization transfer and TROSY during the evolution and acquisition periods. It is the shortest scheme with only one transfer period τ, however, at the cost of no multiplet peak selection and in principle, all four components of a ^{15}N–^{1}H correlation peak are present in the spectrum. In general, only the narrowest peak will be visible in the spectrum, and the three other components will be suppressed by their fast transverse relaxation. In contrast to the CRINEPT schemes, CRIPT suppresses signals from more mobile regions of large proteins and from smaller molecules when the transfer delay is set for detection of very large molecular weights, since the optimal transfer time τ is inversely proportional to the rotational correlation time of the amide moiety.

Water Polarization

In NMR spectra of very large proteins a surprisingly strong dependence of the proton signal intensities on the polarization of the solvent water is observed. The dependence applies over the whole spectral range and not only to some amide ^{1}H resonances for which it is well established that magnetization/saturation transfer can occur from water via amide–proton

the ^{15}N spins is suppressed at the beginning of the sequence by a 90° pulse on ^{15}N followed by G_0. The phase cycles for the experiments are $\phi_1 = (x, -x), \phi_2 = (x, x, -x, -x)$, $\phi_3 = (x, x, x, x, -x, -x, -x, -x)$, and $\phi_4 = (-x, x, x, -x, x, -x, -x, x)$. Quadrature detection in the ^{15}N dimension is achieved using States-TPPI (Marion *et al.*, 1989) applied to the phase ϕ_1. In (A) two free induction decays are recorded for each t_1 increment, with $\psi = \{x, x\}$ and $\psi = \{-x, -x\}$, respectively, and are added with a 90° phase shift in both dimensions (Riek *et al.*, 1999). The duration of the magnetization transfer period τ is typically between 1.5 and 6 ms and decreases with molecular size.

exchange (Bax and Grzesiek, 1993). Moreover, for large compact proteins it is expected that only a minor fraction of the amide protons exchanges at an appreciable rate. In Fig. 3 spectra obtained with different water suppression schemes are compared for a very large protein with 800 kDa molecular weight and a small protein of 6.5 kDa. Only the aliphatic region of the ^{1}H spectrum is shown, excluding the influence of direct effects of amide exchange. The three schemes maintain or temporarily destroy the equilibrium water polarization (Fig. 3). For the small protein, three identical spectra are obtained (Fig. 3C), whereas large differences in intensity are observed in the spectra of the large protein (Fig. 3B), with presaturation producing the least and water flip-back the most signal intensity. But even saturation of the water resonance immediately before acquisition has a

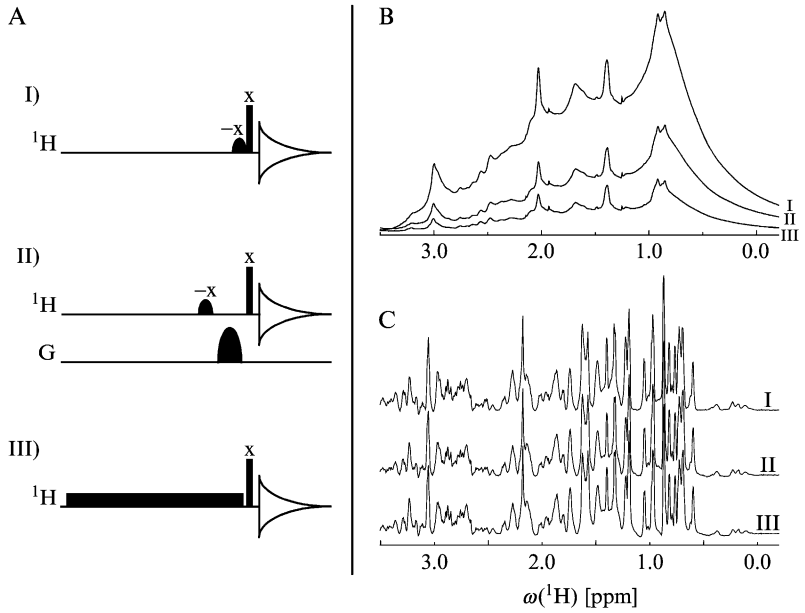

FIG. 3. Aliphatic regions of 1D ^{1}H spectra obtained with experiments using different water suppression techniques. (A) Pulse sequences used: (I) flip-back of water magnetization by a selective 90° pulse at the water frequency with the opposite phase to the 90° broadband excitation pulse directly following; (II) a strong magnetic field gradient pulse is applied between the two pulses described in I; (III) the water resonance is saturated by continuous irradiation of a weak radiofrequency field (presaturation). (B) ^{1}H spectra of GroEL from *E. coli* (molecular weight 800 kDa) and (C) bovine pancreatic trypsin inhibitor (BPTI; 6.5 kDa) measured with the three schemes shown in (A). In the spectra of GroEL, large intensity changes are observed whereas the spectra of BPTI are identical.

large impact. These effects are observed for protonated as well as for perdeuterated proteins studied in H_2O solutions (Hohwy *et al.*, 2004).

The strong coupling between the water protons and the protons in large globular proteins has an additional important consequence. The effective longitudinal relaxation times T_1 of the protein protons strongly depend on the polarization of the water protons. The experiments that conserve the water polarization using water flip-back pulses show the shortest effective T_1 values (Hohwy *et al.*, 2004). The relaxation is much shorter than expected from simple models of relaxation that predict a dramatic increase of T_1 for longer rotational correlation times. The short effective proton longitudinal relaxation times imply that optimal sensitivity is obtained with shorter waiting periods between successive scans than typically used for small proteins, e.g., an interscan period around 0.5 s was found optimal in experiments with the 800-kDa chaperonin GroEL when carefully adjusted water flip-back pulses were used.

The experimental findings were recently explained by a model that predicted and quantified the saturation transfer and the drastic reduction of the longitudinal relaxation times observed (Hohwy *et al.*, 2004). The model shows that fast exchanging hydroxyl groups of the amino acid side chains and internal water molecules are the dominating mechanisms of interaction between water protons and protons in the protein. The hydroxyl groups usually have exchange rates larger than $\sim 250\ s^{-1}$ for all pH values (see Fig. 2.3 in Wüthrich, 1986). These hydroxyl groups are omnipresent in proteins and, for a large fraction of all protons in a protein, hydroxyl groups are found within a distance of 0.5 nm, permitting efficient cross-relaxation. For the case of the 110-kDa protein DHNA (7,8-dihydroneopterin aldolase from *Staphylococcus aureus*), a clear correlation was found between the distance to a hydroxyl proton or an interior water molecule and the strength of interaction between nonexchanging protein protons and water protons: this finding confirms the assumption made in the model (Hohwy *et al.*, 2004).

Water flip-back pulses can never completely restore equilibrium magnetization of water protons. As a result, shorter T_1 relaxation of water would increase its steady-state magnetization and thus improve the quality of the NMR spectra of large proteins. Two conflicting effects have to be optimized: the T_1 of water must be reduced without increasing the transverse relaxation of the protein protons. Recent experiments in our laboratory have shown that this requirement can be fulfilled using chelated paramagnetic ions (Hiller *et al.*, 2004). Such relaxation agents permit access of water molecules to the paramagnetic ion but keep the protein at a large distance, which minimizes relaxation of protein resonances. The T_1 of water can easily be reduced by a factor of 20 and still transverse relaxation

of protons in large proteins is increased by only a few percent. Moreover, it was found that by a proper choice of the paramagnetic additive, full water equilibrium magnetization can be maintained without the use of any water flip-back pulses. This finding is important because a careful adjustment of the flip-back pulses can be tedious, and some experiments, e.g., CRIPT, often show a large residual water resonance compromising spectral quality, which can be markedly improved by temporarily saturating the water resonance.

Experimental Procedures

When performing NMR experiments with very large biological macromolecules some basic aspects require special attention. Even though the resonance lines of the protein are very broad a good homogeneity of the main magnetic field is crucial for an optimal performance of the water flip-back pulses, which depend on the quality of the line shape of the water resonance. Often better shimming is required than for small molecules where residual water can be removed by techniques such as WATERGATE (Piotto *et al.*, 1992). Such sequences can, in general, not be applied with very large molecules because they increase the length of the pulse sequence, which must be kept to an absolute minimum to counteract relaxation.

A further aspect concerns the determination of the length of the radiofrequency pulses. For nuclei other than protons, the pulses can usually be taken from measurements with another sample if the receiver coil can be tuned to the same performance with the sample of interest. For protons this procedure is often not precise enough and the durations of the proton pulses have to be determined using the sample with the large protein. Due to the strong influence of the polarization of the water protons on the protons of the protein, the length of a selective water flip-back pulse and the wideband excitation pulse would have to be determined simultaneously, which is not easily possible. For this reason, the 360° pulse for the water resonance is determined, which again requires good field homogeneity and possibly a susceptibility matched sample tube that eliminates pick-up of signal outside the central region of the receiver coil. Such sample tubes benefit all measurements with very large proteins since better suppression of residual water signals can be obtained.

The importance of the water polarization requires a particularly careful adjustment of the water flip-back pulses. The pulses chosen should not be too selective, which is usually not a limitation since the proteins are deuterated and the water resonance is at an ample distance to the nearest proton resonance of interest (amide protons). A pulse length of about 1 ms

has proven to be adequate at magnetic field strengths corresponding to 800 or 900 MHz proton resonance frequency. Two selective pulses have to be determined (usually they are chosen with the same duration but different powers): one flipping water magnetization from the z-axis into the transverse plane and one flipping it from the transverse plane back to the z-axis. The two pulses differ due to the different influence of the radiation damping effect on the water signal, which counteracts excitation of the water resonance but supports flipping it back to the positive z-axis. The appropriate selective pulses can then be introduced into the pulse sequence of interest.

Before starting the experiment, the phase and power of the selective pulses at the water resonance frequency have to be fine tuned at their specific position in the pulse sequence. Good water suppression has to be obtained, and at the same time maximal water polarization must be maintained. As a final test of the performance of the experiment, the quality of the water flip-back is tested. Applying a very small excitation pulse at the water frequency permits determination of the maximal water magnetization without disturbing it. The same small pulse is then inserted just before the acquisition in the pulse sequence of interest, and the intensity of the water resonance is monitored for the first few evolution time increments (Hohwy *et al*., 2004). The intensity will decrease from the maximal value to a steady-state value that reaches typically between 65 and 90% of the equilibrium value depending on the type of experiment and the number of water flip-back pulses. With this monitoring system, misadjustment can easily be detected.

Before obtaining spectra of a new protein, the polarization transfer periods have to be estimated. The values can be obtained from the molecular weight (Riek *et al*., 2002) or measured using the first free induction decay (FID) of the multidimensional experiment with different transfer periods. For an estimate, the amide regions in the corresponding 1D ^{1}H spectra are integrated and plotted against the polarization transfer delay τ (Fig. 2). Figure 4 shows the results of such build-up measurements with the 2D [^{15}N, ^{1}H]-CRIPT-TROSY sequence (Fig. 2C) applied with the 110-kDa protein DHNA and the 800-kDa GroEL, respectively.

For initial experiments, 2D [^{15}N, ^{1}H]-CRINEPT-HMQC-[^{1}H]-TROSY is often best suited due to its relatively high sensitivity and the combination of INEPT and CRIPT magnetization transfers. However, the resolution is limited in the ^{15}N dimension resulting in broad lines. The evaluation of this first spectrum will then indicate whether CRINEPT or CRIPT experiments are required for the NMR studies. The merits of the different pulse sequences shown in Fig. 2 were previously discussed extensively (Riek *et al*., 2002). Even with relaxation compensation, the resonances are very broad

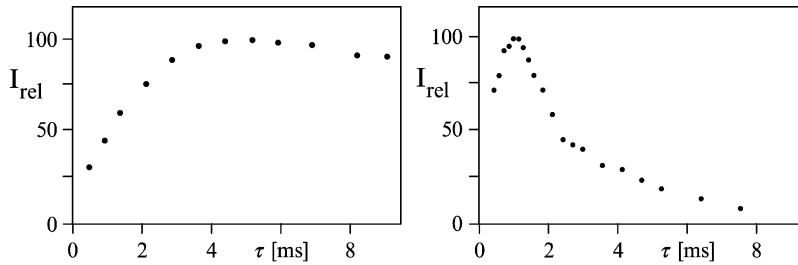

FIG. 4. CRIPT build-up curves for the 110-kDa uniformly $^{15}N,^{2}H$-labeled 7,8-dihydroneopterin aldolase (DHNA) from *Staphylococcus aureus* (left) and the 800-kDa [$^{15}N,^{2}H$]-GroEL from *E. coli* (right). A series of 1D ^{1}H spectra was measured using the 2D [$^{15}N,^{1}H$]-CRIPT experiment (Fig. 2C) with evolution period $t_1 = 0$. The intensity, I_{rel}, is the integral over the resonances in the low-field amide spectral region. The maxima of the two build-up curves were set independently to a value of 100. The optimal CRIPT transfer period for DHNA is about 5 ms and for GroEL it is about 1.5 ms.

in CRIPT and CRINEPT spectra, reminiscent of the broad lines in absolute value spectra, requiring stronger window functions (Wider *et al.*, 1984). Often, the data have to be transformed with different window functions to make different features of the spectra visible. Correspondingly, special consideration has to be given to the choice of the window function used in the processing of the data as described in detail by Riek *et al.* (2002). As an example of a heteronuclear correlation spectrum of a very large protein and of the quality of spectra that can be obtained, Fig. 5 presents a 2D [^{15}N, ^{1}H]-CRIPT-TROSY spectrum of the perdeuterated 800-kDa tetradecameric chaperonin GroEL from *Escherichia coli*. The experimental details are given in the figure caption. A 2D [$^{15}N,^{1}H$]-TROSY spectrum of GroEL contains very few resonances from more mobile regions in the protein (Riek *et al.*, 2002) and does not show the typical pattern of a folded protein as observed in the spectrum in Fig. 5.

Perspective

With novel NMR techniques correlation spectra of biological macromolecules up to 1 MDa can be acquired in solution. These methods were already successfully applied to study large proteins (Fernández and Wider, 2003; Fiaux *et al.*, 2002; McElroy *et al.*, 2002; Rudiger *et al.*, 1999; Salzmann *et al.*, 2000; Tugarinov *et al.*, 2002). With increasing molecular weight of the proteins under investigation, the number of polarization transfer steps and the overall duration of the experimental schemes must be reduced.

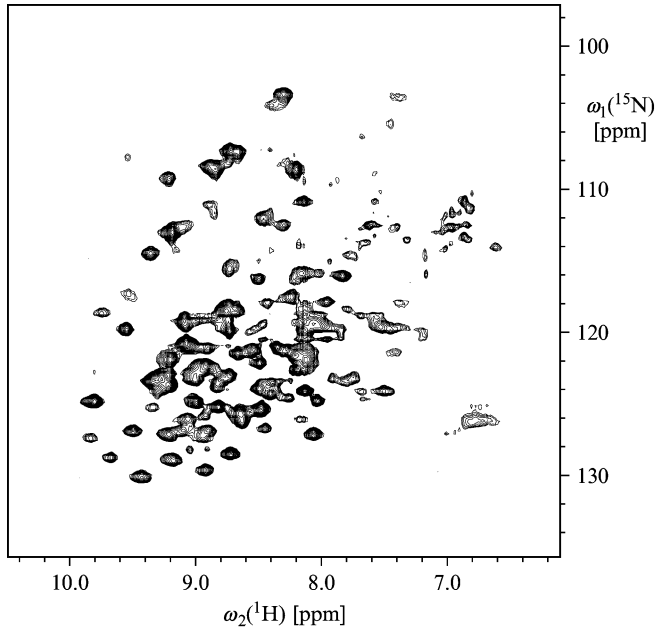

FIG. 5. 2D [^{15}N,^{1}H]-CRIPT-TROSY spectrum of a 1.5 m*M* sample of perdeuterated and ^{15}N-labeled 800-kDa tetradecameric GroEL containing 20 m*M* KCl and 25 m*M* phosphate buffer at pH 6.2, $T = 35^{\circ}$, measured at 750 MHz using the experimental scheme shown in Fig. 2C. The CRIPT transfer period was 1.6 ms, the maximal evolution time 16 ms, the interscan delay 300 ms, the acquisition time 95 ms, and the total measuring time 12 h; 72 and 1024 complex points were measured in the evolution and in the acquisition periods, respectively; before Fourier transformation the data were multiplied with a sine bell shifted by 20° in the indirect dimension and an exponential function in the direct dimension, zero-filling to 256 times 2048 data points, was applied (Wider *et al.*, 1984). The resulting spectrum was baseline corrected in both dimensions.

Measurements of magnetization transfer efficiencies in the 110-kDa protein DHNA (Braun *et al.*, 2003) indicate that TROSY-type triple resonance experiments (Salzmann *et al.*, 1998, 1999; Yang and Kay, 1999) or experiments with relayed magnetization transfer steps will become increasingly difficult with the current technology when applied to proteins with molecular weights beyond 200–300 kDa (Chung and Kroon, 2003). Triple resonance experiments are usually the basis for sequence-specific resonance assignments, which are the foundation for a detailed analysis of the spectra. When these experiments fail, alternative methods must be developed. A promising approach seems to be the use of experiments based on nuclear Overhauser enhancements (NOEs). Initial studies with a 500-kDa

protein complex support this idea and permitted the assignment of resonances (R. Horst, unpublished observations).

The amide resonances provide a wealth of information with which to characterize a protein. Still, it may be desirable to obtain information on amino acid side chains. A promising approach seems to be the protonation of some methyl groups in an otherwise perdeuterated protein. This procedure has been shown to be very successful in obtaining more information in large molecules (Fernández *et al*., 2004; Mueller *et al*., 2000) and seems to provide signals in very slowly tumbling molecules (Kreishman-Deitrick *et al*., 2003). Again, the assignment of the methyl group resonances may have to rely on NOEs, since through-bond correlation experiments (Hilty *et al*., 2002; Tugarinov and Kay, 2003) most likely will not be sensitive enough with very large molecules. In the future, further applications of TROSY, CRINEPT, and CRIPT will answer questions related to the structure and function of supramolecular structures such as membrane proteins solubilized in micelles or lipid vesicles, proteins attached to nucleic acid fragments, or oligomeric proteins. The methodology will be supported by new isotope labeling techniques for proteins and nucleic acids and further advances in NMR technology.

Acknowledgments

I thank Dr. Reto Horst for discussions on all aspects of NMR spectroscopy with very large biological macromolecules, Sebastian Hiller for providing the data for Fig. 3, and Prof. Kurt Wüthrich for his continuous support and interest in my research.

References

Bax, A., and Grzesiek, S. (1993). Methodological advances in protein NMR. *Acc. Chem. Res.* **26,** 131–138.

Braun, D., Wüthrich, K., and Wider, G. (2003). Dissection of heteronuclear NMR experiments for studies of magnetization transfer efficiencies. *J. Magn. Reson.* **165,** 89–94.

Brüschweiler, R., and Ernst, R. R. (1992). Molecular dynamics monitored by cross-correlated cross relaxation of spins quantized along orthogonal axes. *J. Chem. Phys.* **96,** 1758–1766.

Brutscher, B., Boisbouvier, J., Pardi, A., Marion, D., and Simorre, J. P. (1998). Improved sensitivity and resolution in ^{1}H–^{13}C NMR experiments of RNA. *J. Am. Chem. Soc.* **120,** 11845–11851.

Chung, J., and Kroon, G. (2003). ^{1}H, ^{15}N, ^{13}C-triple resonance NMR of very large systems at 900 MHz. *J. Magn. Reson.* **163,** 360–368.

Dalvit, C. (1992). ^{1}H to ^{15}N polarization transfer via ^{1}H CSA–^{1}H-^{15}N dipole dipole cross correlation. *J. Magn. Reson.* **97,** 645–650.

Fernández, C., and Wider, G. (2003). TROSY in NMR studies of the structure and function of large biological macromolecules. *Curr. Opin. Struct. Biol.* **13,** 570–580.

Fernández, C., Hilty, C., Wider, G., Güntert, P., and Wüthrich, K. (2004). NMR structure of the integral membrane protein OmpX. *J. Mol. Biol.* **336,** 1211–1221.

Fiaux, J., Bertelsen, E. B., Horwich, A. L., and Wüthrich, K. (2002). NMR analysis of a 900K GroEL–GroES complex. *Nature* **418,** 207–211.

Fushman, D., and Cowburn, D. (1999). The effect of noncolinearity of ^{15}N-^{1}H dipolar and ^{15}N CSA tensors and rotational anisotropy on ^{15}N relaxation, CSA/dipolar cross correlation, and TROSY. *J. Biomol. NMR* **13,** 139–147.

Gardner, K. H., and Kay, L. E. (1998). The use of ^{2}H, ^{13}C, ^{15}N multidimensional NMR to study the structure and dynamics of proteins. *Annu. Rev. Biophys. Biomol. Struct.* **27,** 357–406.

Goldman, M. (1984). Interference effects in the relaxation of a pair of unlike spin-1/2 nuclei. *J. Magn. Reson.* **60,** 437–452.

Hiller, S., Wider, G., Etezady-Esfarjani, T., Horst, R., and Wüthrich, K. (2004). Managing the solvent water polarization to obtain improved NMR spectra of large molecular structures. *J. Biomol. NMR.* Submitted.

Hilty, C., Fernández, C., Wider, G., and Wüthrich, K. (2002). Side chain NMR. assignments in the membrane protein OmpX reconstituted in DHPC micelles. *J. Biomol. NMR* **23,** 289–301.

Hohwy, M., Braun, D., and Wider, G. (2004). Characterization of the influence of protein-water interactions on the NMR spectra of large proteins. *J. Biomol. NMR.* Submitted.

Kainosho, M. (1997). Isotope labelling of macromolecules for structural determinations. *Nat. Struct. Biol.* **4,** 858–861.

Kreishman-Deitrick, M., Egile, C., Hoyt, D. W., Ford, J. J., Li, R., and Rosen, M. K. (2003). NMR analysis of methyl groups at 100–500 kDa: Model systems and Arp2/3 complex. *Biochemistry* **42,** 8579–8586.

Lian, L. Y., and Middleton, D. A. (2001). Labelling approaches for protein structural studies by solution-state and solid-state NMR. *Prog. NMR Spectrosc.* **39,** 171–190.

Marion, D., Ikura, M., Tschudin, R., and Bax, A. (1989). Rapid recording of 2D NMR spectra without phase cycling. Application to the study of hydrogen exchange in proteins. *J. Magn. Reson.* **85,** 393–399.

McElroy, C., Manfredo, A., Wendt, A., Gollnick, P., and Foster, M. (2002). TROSY-NMR studies of the 91 kDa TRAP protein reveal allosteric control of a gene regulatory protein by ligand-altered flexibility. *J. Mol. Biol.* **323,** 463–473.

Morris, G. A., and Freeman, R. (1979). Enhancement of NMR signals by polarization transfer. *J. Am. Chem. Soc.* **101,** 760–762.

Mueller, G. A., Choy, W. Y., Yang, D., Forman-Kay, J. D., Venters, R. A., and Kay, L. E. (2000). Global folds of proteins with low densities of NOEs using residual dipolar couplings: Application to the 370-residue maltodextrin-binding protein. *J. Mol. Biol.* **300,** 197–212.

Müller, L. (1979). Sensitivity enhanced detection of weak nuclei using heteronuclear multiple quantum coherence. *J. Am. Chem. Soc.* **101,** 4481–4484.

Pervushin, K. (2000). Impact of transverse relaxation optimized spectroscopy (TROSY) on NMR as a technique in structural biology. *Q. Rev. Biophys.* **33,** 161–197.

Pervushin, K., Riek, R., Wider, G., and Wüthrich, K. (1997). Attenuated T_2 relaxation by mutual cancellation of dipole-dipole coupling and chemical shift anisotropy indicates an avenue to NMR structures of very large biological macromolecules in solution. *Proc. Natl. Acad. Sci. USA* **94,** 12366–12371.

Pervushin, K., Riek, R., Wider, G., and Wüthrich, K. (1998). Transverse relaxation-optimized spectroscopy (TROSY) for NMR studies of aromatic spin systems in ^{13}C-labeled proteins. *J. Am. Chem. Soc.* **120,** 6394–6400.

Piotto, M., Saudek, V., and Sklenar, V. (1992). Gradient-tailored excitation for single quantum NMR spectroscopy of aqueous solutions. *J. Biomol. NMR* **2,** 661–665.

Riek, R., Wider, G., Pervushin, K., and Wüthrich, K. (1999). Polarization transfer by cross-correlated relaxation in solution NMR with very large molecules. *Proc. Natl. Acad. Sci. USA* **96,** 4918–4923.

Riek, R., Fiaux, J., Bertelsen, E. B., Horwich, A. L., and Wüthrich, K. (2002). Solution NMR techniques for large molecular and supramolecular structures. *J. Am. Chem. Soc.* **124,** 12144–12153.

Rudiger, S., Freund, S. M. V., Veprintsev, D. B., and Fersht, A. R. (1999). CRINEPT-TROSY NMR reveals p53 core domain bound in an unfolded form to the chaperone Hsp90. *Proc. Natl. Acad. Sci. USA* **99,** 11085–11090.

Salzmann, M., Pervushin, K. G., Wider, G., Senn, H., and Wüthrich, K. (1998). TROSY in triple-resonance experiments: New perspectives for sequential NMR assignment of large proteins. *Proc. Natl. Acad. Sci. USA* **95,** 13585–13590.

Salzmann, M., Wider, G., Pervushin, K., Senn, H., and Wüthrich, K. (1999). TROSY-type triple-resonance experiments for sequential assignments of large proteins. *J. Am. Chem. Soc.* **121,** 844–848.

Salzmann, M., Pervushin, K., Wider, G., Senn, H., and Wüthrich, K. (2000). NMR assignment and secondary structure determination of an octameric 110 kDa protein using TROSY in triple resonance experiments. *J. Am. Chem. Soc.* **122,** 7543–7548.

Shuker, S. B., Hajduk, P. J., Meadows, R. P., and Fesik, S. W. (1996). Discovering high-affinity ligands for proteins: SAR by NMR. *Science* **274,** 1531–1534.

Tugarinov, V., and Kay, L. E. (2003). Ile, Leu, and Val methyl assignments of the 723-residue malate synthase G using a new labeling strategy and novel NMR methods. *J. Am. Chem. Soc.* **125,** 13868–13878.

Tugarinov, V., Muhandiram, R., Ayed, A., and Kay, L. E. (2002). Four-dimensional NMR spectroscopy of a 723-residue protein: Chemical shift assignments and secondary structure of malate synthase G. *J. Am. Chem. Soc.* **124,** 10025–10035.

Tugarinov, V., Hwang, P. M., Ollerenshaw, J. E., and Kay, L. E. (2003). Cross-correlated relaxation enhanced ^{1}H-^{13}C NMR spectroscopy of methyl groups in very high molecular weight proteins and protein complexes. *J. Am. Chem. Soc.* **125,** 10420–10428.

Wider, G. (1998). Technical aspects of NMR spectroscopy with biological macromolecules and studies of hydration in solution. *Prog. NMR Spectrosc.* **32,** 193–275.

Wider, G., and Wüthrich, K. (1999). NMR spectroscopy of large molecules and multimolecular assemblies in solution. *Curr. Opin. Struct. Biol.* **9,** 594–601.

Wider, G., Macura, S., Kunar, A., Ernst, R. R., and Wüthrich, K. (1984). Homonuclear two-dimensional ^{1}H NMR of proteins. Experimental procedures. *J. Magn. Reson.* **56,** 207–234.

Wüthrich, K. (1986). ''NMR of Proteins and Nucleic Acids.'' Wiley, New York.

Wüthrich, K., and Wider, G. (2003). Transverse relaxation-optimized NMR spectroscopy with biomacromolecular structures in solution. *Magn. Reson. Chem.* **41,** S80–S88.

Xu, R., Ayers, B., Cowburn, D., and Muir, T. W. (1999). Chemical ligation of folded recombinant proteins: Segmental isotopic labeling of domains for NMR studies. *Proc. Natl. Acad. Sci. USA* **96,** 388–393.

Yamazaki, T., Otomo, T., Oda, N., Kyogoku, Y., Uegaki, K., Ito, N., Ishino, Y., and Nakamura, H. (1998). Segmental isotope labeling for protein NMR using peptide splicing. *J. Am. Chem. Soc.* **120,** 5591–5592.

Yang, D., and Kay, L. E. (1999). TROSY triple-resonance four-dimensional NMR spectroscopy of a 46 ns tumbling protein. *J. Am. Chem. Soc.* **121,** 2571–2575.

Yu, H. T. (1999). Extending the size limit of protein nuclear magnetic resonance. *Proc. Natl. Acad. Sci. USA* **96,** 332–334.